Origin, evolution and dynamic context of a Neoglacial lateral-frontal moraine at Austre Lovénbreen, Svalbard

Nicholas G. Midgley[a]*, Simon J. Cook[b], David J. Graham[c] and Toby N. Tonkin[a]

[a] School of Animal, Rural and Environmental Sciences, Nottingham Trent University, Brackenhurst Campus, Southwell, Nottinghamshire, NG25 0QF, UK.

[b] School of Science and the Environment, Manchester Metropolitan University, Chester Street, Manchester, M1 5GD, UK.

[c] Polar and Alpine Research Centre, Department of Geography, Loughborough University, Leicestershire, LE11 3TU, UK.

Keywords: debris-rich basal glacier ice, ground-penetrating radar, moraine, Svalbard

* Corresponding author. Tel.: +44 1636 817 016; fax: +44 1636 817 066.

E-mail address: nicholas.midgley@ntu.ac.uk

Abstract

Moraines marking the Neoglacial limits in Svalbard are commonly ice cored. Investigating the nature of this relict ice is important because it can aid our understanding of former glacier dynamics. This paper examines the composition of the lateral-frontal moraine associated with the Neoglacial limit at Austre Lovénbreen and assesses the likely geomorphological evolution. The moraine was investigated using ground-penetrating radar (GPR), with context being provided by structural mapping of the glacier based on an oblique aerial image from 1936 and vertical aerial imagery from 2003. Multiple up-glacier dipping reflectors and syncline structures are found in the GPR surveys. The reflectors are most clearly defined in lateral positions, where the moraine is substantially composed of ice. The frontal area of the moraine is dominantly composed of debris. The core of the lateral part of the moraine is likely to consist of stacked sequences of basal ice that have been deformed by strong longitudinal compression. The long term preservation potential of the ice-dominated lateral moraine is negligible, whereas the preservation of the debris-dominated frontal moraine is high. A glacier surface bulge, identified on the 1936 aerial imagery, provides evidence that Austre Lovénbreen has previously displayed surge activity, although it is highly unlikely to do so in the near future in its current state. This research shows the value of relict buried ice that is preserved in landforms to aiding our understanding of former glacier characteristics.

1. Introduction

The aim of this research is to investigate the origin of buried glacier ice within the lateral-frontal moraine of Austre Lovénbreen, Svalbard (Fig. 1), and to assess the evolution and preservation potential of this landform as the ice core degrades over time. To achieve this aim, a detailed ground-penetrating radar (GPR) survey was used to determine the internal architecture and composition of the moraine and ice core, and set this within the structural and dynamic context of the glacier by undertaking glacier structural mapping from contemporary vertical aerial and historic oblique aerial imagery. The ice core within the moraine preserves potentially valuable palaeoglaciological information from the Neoglacial maximum, which combined with structural mapping, extends recent work in the region that has examined changing glacier characteristics and dynamics (Hambrey et al., 2005). Such work is necessary in order to contextualise glacier change in the Arctic, a region which has experienced exceptional rates of warming in recent decades (IPCC, 2007). In addition, landforms at contemporary glaciers are commonly used as analogues for the interpretation of mid-latitude Pleistocene glacial landforms, so a fuller understanding of the formation and post-formational evolution of moraines in contemporary settings such as this can also aid our understanding of previously glaciated settings.

2. Research context

The lateral and frontal moraines formed at the Neoglacial maximum limits in Svalbard are often considered to be ice-cored (e.g. Glasser and Hambrey,

2003). Lateral moraines have traditionally been considered to have formed by the accumulation of thin layers of coarse angular debris on top of a thick glacier ice accumulation (e.g. Flint, 1971; Embleton and King, 1975; Sugden and John, 1976; Boulton and Eyles, 1979). According to this model, lateral moraines have low preservation potential during deglaciation as the ice would ablate quickly under a thin debris cover. The term has also been used to refer to both moraines that are detached from the glacier and to thin debris covers at the margins of active glacier ice. Where the debris cover in ice-cored lateral moraines is both thin and contains a significant component of fine-grained sediment, the debris cover is prone to reworking and exposure of the relict glacier ice. Where the debris cover allows, an ice-core can form a relatively stable part of the landform. Ice-cored lateral-frontal moraines have been reported from a number of glaciers in Svalbard, including: Scott Turnerbreen (Lønne and Lauritsen, 1996); Kongsvegen (Bennett et al., 2000); Longyearbreen and Larsbreen (Etzelmüller et al., 2000; Lukas et al., 2005); Rieperbreen (Lysså and Lønne, 2001); Platåbreen (Lønne and Lysså, 2005); Platåbreen / Nordenskiöldtoppenbreen (Lukas et al., 2005); Holmströmbreen (Schomaker and Kjær, 2008); and Ragnarbreen (Ewertowski et al., 2012).

The use of the term ice-cored moraine has also caused some debate with Lukas et al. (2007) arguing for a strict application of the term with detachment from the glacier needed to justify its application. A more pragmatic use of the ice-cored moraine term has also been reasoned for (Lønne, 2007; Evans, 2009) with the term not needing to indicate detachment from a glacier.

90 Evans' (2009) work on *controlled moraine* formation highlights the 'linearity'
91 that is found in landforms associated with incorporated ice. This linearity can,
92 typically, be seen on aerial images (e.g. the western end of the outer moraine
93 in Fig. 2) and serves as a useful and simple diagnostic criterion for the
94 recognition of potential ice-cored character.

95 Investigation of ice-cored moraines can potentially aid our understanding of
96 former glacier characteristics and any associated climatic significance. The ice
97 core within such moraine complexes may include glacier ice, basal ice, or a
98 combination of both. At modern ice margins, basal ice may record important
99 information about prevailing conditions and the processes operating in the
100 inaccessible subglacial environment further up-glacier (Hubbard and Sharp,
101 1989; Knight, 1997; Hubbard et al., 2009). Evidence for tectonic deformation
102 of the ice-core sequence (i.e. folds and thrusts) could also indicate a range of
103 dynamic and flow conditions when the ice was part of the parent glacier. For
104 example, englacial thrusts and folds have been inferred to indicate flow
105 compression either as a result of polythermal glacier conditions (e.g. Hambrey
106 et al., 1999), ice flow against a steep reverse bedslope (e.g. Swift et al., 2006),
107 or during glacier surges (e.g. Sharp et al., 1994; Waller et al., 2000). Some of
108 these basal ice characteristics may also be preserved in the moraine sediment
109 as the basal ice melts, offering the potential to reconstruct basal ice
110 characteristics from deglaciated terrain (e.g. Evans, 2009; Knight et al., 2000;
111 Cook et al., 2011).

112 Recent work by Hambrey et al. (2005) at neighbouring Midtre Lovénbreen
113 highlighted the value of glacier structural mapping in developing an

114 understanding of the changing dynamics of glaciers in the context of climatic
115 warming. The work of Hambrey et al. (2005) remains, however, an isolated
116 example of how analysis of temporally separated aerial and oblique aerial
117 imagery can be used to evaluate glaciological change over time. Our study
118 extends the record of changing glacier dynamics in this region, and thereby
119 contributes to a broader understanding of both glacier and climatic change in
120 the region. In particular, and as highlighted in the study of Midtre Lovénbreen,
121 there is some uncertainty about whether the Lovénbreen glaciers experience
122 surge-type behaviour (Hambrey et al., 2005). Ground-based imagery of these
123 glaciers by Hamberg (1894) from 1892 showed near-vertical ice cliffs at their
124 Neoglacial moraines. This feature was interpreted by Liestøl (1988) to indicate
125 surging. Hagen et al. (1993) also classify Midtre Lovénbreen as a surge-type
126 glacier. Later work by Jiskoot et al. (2000) indicated that these glaciers were
127 not surge-type, whereas Hansen (2003) suggested that Midtre Lovénbreen had
128 surged in the past, but could no longer be classified as a surge-type glacier. On
129 the basis of structural analysis, Hambrey et al. (2005) also concluded that
130 Midtre Lovénbreen was not a surge-type glacier, or at least had not surged for
131 several hundred years. Recognition of surge-type behaviour has important
132 implications for understanding their behaviour in the context of climatic change,
133 since glacier surges may lead to advance even during climatic amelioration.
134 Little is known about whether Austre Lovénbreen has experienced surging
135 behaviour in the past, but our analysis of historical and modern aerial imagery,
136 as well as the structures preserved within the ice-core of the Neoglacial
137 moraine, contributes to our understanding of the dynamics of this glacier.

3. Study area

Austre Lovénbreen (78°53’12’’N 12°08’50’’E) is located near Ny-Ålesund on Brøggerhalyøva on the island of Spitsbergen, part of the Svalbard archipelago, in the Norwegian high-Arctic (Fig. 1). Austre Lovénbreen is a small valley glacier that was around 5 km in length at its Neoglacial maximum, but is currently just less than 4 km in length.

The thermal regime of Austre Lovénbreen in 2010 was polythermal, based on our interpretation of GPR profiles undertaken in 2010 by Saintenoy et al. (2013), albeit with an extensive region of cold-based ice and an exceptionally small region of warm-based ice at the deepest part of the glacier. The longitudinal profile of the Austre Lovénbreen bed, again based on our interpretation of GPR profiles undertaken by Saintenoy et al. (2013), also highlights an overdeepening starting at around 250 m and extending to around 2.7 km up-glacier from the 2010 glacier terminus (Fig. 4 in Saintenoy et al., 2013). At the adjacent polythermal Midtre Lovénbreen, previous research has highlighted up-glacier migration of the boundary between cold- and warm-based ice that was identified from GPR surveys undertaken in 1998 and 2006 (Rippin et al., 2007). Evolution of the thermal regime in response to climatic warming and thinning of the ice is also recognised at other Svalbard glaciers (e.g. Hodgkins et al., 1999).

In common with other glaciers in the area, the glacier terminus of Austre Lovénbreen has receded by around 1 km since the Neoglacial maximum extent

161 at the end of the nineteenth century. The adjacent Midtre and Vestre
162 Lovénbreen were photographed by Hamberg (1894) in 1892 with high, near-
163 vertical ice margins, at what is now probably the outer part of the moraine-
164 mound complex surrounding each glacier. Given that Austre Lovénbreen is
165 comparable to these glaciers in most respects, it seems likely that it exhibited
166 similar features and reached its Neoglacial maximum at around the same time.
167 The photographic evidence of the Lovénbreen glaciers also corresponds with
168 the work by Svendsen and Mangerud (1997) on the response of Linnébreen in
169 central Spitsbergen indicating Neoglacial distal moraine formation during the
170 late nineteenth century. Overridden soil and vegetation, now found beneath
171 the nearby Longyearbreen, indicate that *c*. 1100 years ago the margin of the
172 glacier was at least 2 km upstream of the current margin (Humlum et al.,
173 2005). As this glacier is typical of central Spitsbergen glaciers in terms of
174 topographic setting, aspect and size (Humlum et al., 2005), it seems likely that
175 Austre Lovénbreen has experienced a similar advance and recession to that of
176 Longyearbreen over a timescale of over 1100 years.

177 The continuing terminus recession of Austre Lovénbreen is associated with the
178 typically negative mass balance of the glacier that is demonstrated by the
179 mass balance record from 1968 to 2009 at the adjacent Midtre Lovénbreen
180 (WGMS, 2011). Friedt et al. (2012) show the Austre Lovénbreen glacier front
181 positions mapped in 1962, 1995 and 2009. Between 1962 and 1995 the glacier
182 receded by ~300 m, and between 1995 and 2009 the glacier receded by
183 ~75 m.

184 The moraine complex in front of Austre Lovénbreen consists of well-developed
185 high-relief (*c*. 30–60 m high) lateral moraines, completely detached from the
186 glacier, which continue and merge into the frontal outer moraine complex (*c*.
187 10 m high) with a distinct difference in morphology to the low-relief
188 (commonly around 5 m high) 'hummocky moraine' areas within the moraine-
189 mound complex (Fig. 2).

190 The west coast of Spitsbergen experiences a much warmer climate than its
191 79°N location might imply, with Ny-Ålesund having a mean annual
192 temperature of –6.3 °C from 1961 to 1990 and –5.2 °C from 1981 to 2010
193 (Førland et al., 2011).

194

195 **4. Methods**

196 A pulseEKKO Pro ground-penetrating radar (GPR) system was used with a
197 400 V transmitter and 100 MHz centre frequency antennae to investigate the
198 subsurface characteristics along a series of transects over the outer lateral-
199 frontal moraine complex of Austre Lovénbreen (see Fig. 2B for transect
200 locations). The fieldwork was undertaken during winter conditions in April 2012
201 to ensure the presence of frozen ground. The moraines were covered with a
202 surface ice layer (where this ice layer was visible, it was typically ~5 cm thick)
203 and overlying snow. Whilst snow depth was spatially variable, based upon 45
204 measurements taken at fixed interval along the transects, snow depth was
205 generally less than 5 cm, but was exceptionally as deep as 88 cm. Whilst the
206 majority of the outer moraine had limited snow cover, it was not possible to

survey complete transects through and beyond the moraine limits. This was because the prevailing wind through Kongsfjorden at the time the research was undertaken had resulted in deep snow and the formation of large cornices on the NW side of the moraines, which combined with the steep slope of the ice-distal outer moraine face, made both topographic and radar surveys impossible to complete on the ice-distal faces. The 100 MHz antennae were used with the standard 1 m separation and a 0.25 m step size along each transect. A 750 ns time window was used, along with 36 stacks and each trace was manually triggered with the transmitter and receiver stationary and positioned along a 100 m tape. A perpendicular broadside antennae configuration was used with each transect transverse to the moraine ridge crest orientation. The GPR control unit was positioned at least 5 m away from the transmitter and receiver to mitigate any potential signal interference. Velocity was calibrated along each transect with common mid-point (CMP) surveys orientated perpendicular to the main transect (and parallel to the moraine crest). Because the field interpretation of the main reflection-mode transects was that of dipping reflectors, reflection surveys were also undertaken along the line of the CMP surveys to ensure that the CMP survey lines were, as far as possible, parallel to the strike and normal to the direction of dip of the reflectors. The separation distance of the antennae that was completed on each CMP survey was dependent upon the substrate conditions, and ranged from 26–40 m separation, with 40 m being the limit of the fibre optic cable length. An automatic level was used to survey height change along each transect so that the topography could be applied to the radar profiles.

231 Radar profiles were produced using the EKKO_View Deluxe software from
232 Sensors and Software. Dewow, an automatic gain control and topography were
233 applied to each data set during post-processing. A total of 9 reflection-mode
234 main surveys and an additional 17 CMP-mode surveys were obtained around
235 the Austre Lovénbreen lateral-frontal complex.

236 Structural mapping of the glacier surface was undertaken from two images.
237 The first is a monochrome oblique aerial image from 1936 obtained by Norsk
238 Polarinstitut. The second image is an orthorectified aerial image of the lower
239 ~2 km of the glacier tongue and its proglacial area obtained by the NERC ARSF
240 (Natural Environment Research Council, Airborne Research and Survey Facility)
241 in 2003. The 2003 image was derived from 8 scanned true colour contact
242 prints with a resulting spatial resolution of around 1 m.

243

244 **5. Results**

245 *5.1. CMP surveys*

246 The CMP surveys that cross transects 1–5 show ground velocity characteristics
247 that range from 0.16–0.17 m ns^{-1} (Table 1). CMP surveys that cross transects
248 6–7 have a velocity of 0.15 m ns^{-1}, whereas CMP surveys that cross transects
249 8–9 show ground velocity characteristics that range from 0.13–0.14 m ns^{-1}
250 (Table 1). As an example, Fig. 3a shows a CMP survey across transect 2 with
251 an initial air wave of 0.3 m ns^{-1}, a ground wave around 0.22 m ns^{-1} through
252 the snow and a subsurface velocity of 0.17 m ns^{-1}. In contrast, Fig. 3b shows a

253 CMP survey across transect 9 with an initial air wave and a subsurface velocity
254 of 0.13 m ns^{-1}.

255

256 *5.2. Internal structure of the moraine*

257 Multiple up-glacier dipping reflectors that intersect both the ice-proximal and
258 ice-distal faces of the moraine are found in all transects (Figs. 4 and 5). These
259 reflectors are common in transect 1, abundant in transects 2–6 and isolated
260 examples occur in transects 7–9 (Figs. 4 and 5 and Table 2). The reflectors
261 often have an asymptotic profile where the dip become progressively shallower
262 at depth; a characteristic that is shown with particular clarity in transect 2
263 (Figs. 4 and 5). The apparent angle of dip of the reflectors at the intersection
264 of the ground surface ranges from 6–50° (Table 3). The reflector apparent dip
265 angles appear reasonably consistent through transects 2–6, with a dominant
266 41–50° range. However, transect 1 shows lower apparent dip angles with an
267 11–20° dominant range. Transects 7 and 9 are distinct from the other profiles
268 with lower dip angles dominantly within the 20–39° range, but also including
269 examples below 10°, and transect 8 has a dominant range of 31–40°. Transect
270 6 very clearly demonstrates an open syncline structure of reflectors dipping
271 up-glacier in the distal part of the moraine and dipping down-glacier in the
272 proximal part of the moraine (Figs. 4 and 5). This syncline structure is also
273 found in transects 1, 3–4 and 5, but is shown in these examples with less
274 clarity than in transect 6. Transects 7–9 show a number of surface parallel
275 reflectors below the air and surface wave of the GPR profiles (Figs. 4 and 5).

276

277 *5.3. Hyperbolae from point targets*

278 A hyperbolic curve developed over sequential radar traces is created by a point
279 target. Hyperbolae are rare in transects 2–5, in contrast to transects 1 and 6
280 that show a greater number of hyperbolae (Table 2). The dipping reflectors in
281 transects 1 and 6 are, to an extent, slightly obscured by these numerous point
282 hyperbolae. The GPR transects did not have a migration process applied
283 because the dipping tails of each hyperbola can be clearly differentiated from
284 the dipping reflectors. Transects 7–9 reveal a markedly different radar facies
285 that are characterised by multiple overlapping hyperbolae and a lack of clearly
286 identifiable reflectors, in contrast to the surveys along transects 1–6.

287

288 *5.4. Signal attenuation*

289 Transects 1–5 each show clearly identifiable reflector layers down to 15 m
290 depth and in some places down to 20 m depth associated with low signal
291 attenuation (Table 2). Penetration in transect 6 is slightly reduced at 10–15 m
292 depth, but transects 7–9 are markedly different with a lack of clarity below 5 m
293 and an absence of clarity below 10 m depth associated with high signal
294 attenuation (Table 2).

295

296 *5.5 Glacier structural mapping*

297 An assessment of the structural composition of Austre Lovénbreen in 1936 has
298 been undertaken using oblique aerial imagery (Fig. 6). The lowermost ~1 km

299 of the terminus is mapped in greater detail since it is nearer to the viewer and
300 hence the structures more readily identified. In 1936 the glacier had barely
301 receded from its Neoglacial maximum position, although the flat terminus
302 where the glacier met the moraine indicates that it had experienced thinning at
303 the terminus. This is in contrast to the steep terminal ice cliffs described by
304 Hamberg (1894) when the area was visited in 1892.

305 A number of structural features are identified (Fig. 6). Primary stratification is
306 produced originally by snow accumulation in horizontal layers and is found: (1)
307 within one flow unit of the glacier that has been deformed into a nested set of
308 arcuate bands; and (2) as bands stretching across much of the frontal margin,
309 although best developed on the true left of the glacier (Fig. 6).

310 The longitudinal features stretching up-glacier from the ice margin are
311 interpreted as longitudinal foliation. This structure appears around much of the
312 glacier margin, although there are clear concentrations of longitudinal foliation
313 which appear to have released significant quantities of sediment onto the
314 glacier surface.

315 There are also isolated debris-laden fractures in the upper true left terminus.
316 The precise origin of these features is uncertain, but they could represent
317 debris-filled crevasse traces, debris-rich primary stratification, or englacial
318 thrust faults laden with basal sediment.

319 One intriguing feature of the 1936 imagery is a bulge in the glacier surface
320 from the true left valley side across around two thirds of the glacier width
321 (indicated by the thick dotted line on Fig. 6). This bulge is best identified by

322 tracing the prominent longitudinal foliation up-glacier and the slope of the true
323 left lateral margin. The origin and significance of this bulge is uncertain, but it
324 would be consistent with a surge wave propagating down-glacier in 1936.

325 The quality of the 2003 aerial imagery allows a much more detailed structural
326 assessment of Austre Lovénbreen to be mapped (Fig. 7). Three primary flow
327 units are identified, defined by dense areas of longitudinal foliation that can be
328 traced as far up-glacier as the imagery presented permits. These may
329 represent medial moraines produced at the confluence of individual flow units.

330 Primary stratification is a prominent feature in the 2003 imagery and is
331 seemingly more extensive than is shown in the 1936 image. Much of the
332 primary stratification is folded, indicating lateral compression, and where it can
333 be picked out along the trace of longitudinal foliation, is shown to be tightly
334 folded with the fold limbs extending along the axis of flow. Primary
335 stratification is generally less folded in the true left flow unit.

336 Longitudinal foliation is a ubiquitous feature around the glacier margin where it
337 releases significant quantities of sediment. Many of the foliae melting out on
338 the glacier surface can be traced linearly into the proglacial zone. Although
339 longitudinal foliation is concentrated along medial moraine features at flow unit
340 boundaries (cf. Hambrey and Glasser, 2003), this structure can be traced up-
341 glacier from almost any point from the ice margin. There are significant
342 concentrations of longitudinal foliation along the lateral margins, and through
343 much of the central flow unit.

Debris-bearing fractures are mapped close to the true right margin. It is unclear what the origin of these features could be, as was the case for the 1936 imagery, and we advance the same hypotheses for their origin. Notably, these features do not appear in the same location as in the 1936 imagery.

The higher resolution 2003 image allows the mapping of more subtle features including crevasses and crevasse traces. Open crevasses are generally rare, and most such features mapped are in fact crevasse traces (Fig. 7). The highest density of crevasse traces can be found along the true left flow unit. Crevasse traces are also found along the true right lateral margin, but the density of crevasse-related features here is much lower. Crevasse traces along the true right are relatively short (~150 m in length) compared with the extensive (up to ~500 m long) arcuate crevasse traces across the centre of the glacier terminus.

6. Discussion

6.1. Moraine composition

The CMP surveys revealed radar velocities through the moraine of between 0.13 and 0.17 m ns^{-1}, indicating that its composition is varied. High velocities (at, or close to the 0.17 m ns^{-1} velocity through glacier ice; Murray and Booth, 2010; Saintenoy et al., 2013), combined with low signal attenuation and associated deep penetration, are characteristic of a large ice component (Table 4). Lower velocities and relatively higher signal attenuation are indicative of a significant sediment component. Schwamborn et al. (2008) determined the

radar velocity through unsorted 'outwash [and] morainic deposits' in the proglacial area of the adjacent Midtre Lovénbreen to be 0.127 m ns^{-1}. The sequence at Midtre Lovénbreen, which appears to be mostly clast-rich intermediate diamicton (Fig. 8 in Schwamborn et al., 2008), was just under 3 m thick with a mean ice content of around 10% (gravimetric ice content expressed as water equivalent, as determined from a 6 cm diameter permafrost core) and is a common facies in the proglacial setting of Midtre Lovénbreen (Midgley et al., 2007). Although frozen ground conditions prevented us from directly determining the nature of the sediments within the Austre Lovénbreen lateral moraine, previous work has found clast-rich diamicton to be abundant within this moraine-mound complex (Graham, 2002). Given the consistent geology underlying the two glaciers and the proximity of the sites, it is likely that velocities of around 0.13 m ns^{-1} are indicative of frozen diamicton with around 10% interstitial ice at Austre Lovénbreen. Based upon the known radar velocity through both glacier ice (0.17 m ns^{-1}) consisting of ~100% ice and a known velocity for a proglacial debris facies with ~10% interstitial ice component (0.127 m ns^{-1}), a linear interpolation between these two end members can be used to estimate likely velocities for a range of debris-ice mixes (Table 5).

The observed radar velocities of 0.16 to 0.17 m ns^{-1} across transects 1 to 5 are characteristic of a dominant ice component within the outer moraine complex with up to 20% sediment. Radar velocities along transects 6 and 7 still indicate a significant ice component, but with up to 40% sediment. Radar velocities

along transects 8 and 9 are indicative of a relatively low ice component, with sediment contributing between 60% and 80% of the moraine volume.

6.2. Identification of debris within the substrate

Four distinct zones (A–D) of the lateral-frontal outer moraine complex at Austre Lovénbreen are recognised (Fig. 2) on the basis of both the ice-debris mix and the structural characteristics.

Zone A, whilst having a dominant ice component, does exhibit hyperbolae, which are likely to indicate the presence of isolated coarse-grained clastic material within the ice (Fig. 4). This is in contrast to zone B, which also has a dominant ice component, but appears to lack the isolated coarse-grained component that would cause hyperbolae in the radar profiles (Fig. 4). The measured velocity in zone C of transect 6 is the same as that of transect 7, but a high coarse-grained debris load is inferred for transect 7 that inhibits the identification of any structural features (Fig. 4). This is in contrast to the fine-grained debris load found in transect 6, which results in identification of the clear structural characteristics. Zone D has a dominant coarse-grained debris component shown by the ubiquitous overlapping hyperbolae (Fig. 4).

6.3. Structural glaciology and dynamics of Austre Lovénbreen

The structural mapping of Austre Lovénbreen provides important context that aids the understanding of the conditions under which the lateral-frontal moraine formed. A number of features indicate that the glacier is now far less

dynamic than it would have been during its Neoglacial maximum extent. Most notably, there were few actively forming crevasses in 2003 (Fig. 7), indicating that the glacier is now flowing very slowly. The 1936 imagery (Fig. 6) is not of sufficient resolution to identify crevasses, but there is evidence that Austre Lovénbreen had a surface bulge. Further analysis is required in order to determine whether this was a surge-related expression, but the dense population of fractures (interpreted here mostly as crevasse traces) along the true left side of the glacier, close to the ice margin, indicates that this flow unit was more dynamic in the past.

If there had been a surge around 1936, it will not have contributed ice to the ice-core within the lateral-frontal moraines that are under investigation here. It is possible, however, that a surge may have allowed pushing of the glacier against the lateral-frontal moraine and thereby allowed some deformation of the ice-core. Another possibility is that the glacier surged during its Neoglacial advance and that the ice preserved in the lateral-frontal moraine is derived from such a surge. Hansen (2003) suggested that neighbouring Midtre Lovénbreen had once been a surge-type glacier, but could no longer be considered to be so. We suggest, albeit tentatively, that Austre Lovénbreen may once have been a surge-type glacier, but there is no indication that it has surged since ~1936, nor is there any indication that it will surge again in the near future.

6.4. Origin of ice incorporated within the lateral-frontal moraine

436 The structural maps of Austre Lovénbreen provide important context that aid
437 understanding of the origin of the ice now found within the lateral-frontal
438 moraine. The GPR surveys demonstrate that the ice within the moraine
439 contains a combination of ice and debris arranged in layers, some of which
440 have experienced folding.
441 The up-glacier dipping reflectors with minor folding (Fig. 5) are consistent with
442 the structural characteristics of layered primary stratification, as seen in the
443 1936 oblique aerial image (Fig. 6). Hambrey et al. (2005), for example,
444 showed in a longitudinal GPR profile (i.e. orientated parallel with ice flow) that
445 primary stratification at neighbouring Midtre Lovénbreen dipped up-glacier,
446 and had experienced minor folding. However, primary stratification is not likely
447 to contain the significant quantities of debris revealed by the GPR survey. The
448 layering of primary stratification instead usually results from differences in
449 crystallography and bubble content.
450 Debris-bearing structures exist in the terminus of Austre Lovénbreen that are
451 transverse to flow (Figs. 6 and 7). These structures could represent isolated
452 englacial thrusts. It would, however, also be hard to envisage that these
453 isolated features could explain the dense layering shown in the GPR surveys of
454 the moraine. It could be argued, however, that our mapping, without any
455 ground-truthing of the structures, may have under-represented the number of
456 debris-bearing fractures, including thrusts. In particular, there are numerous
457 arcuate fractures that extend across much of the lower part of the terminus,
458 some of which may include thrusts. Indeed, Hambrey et al. (2005) interpreted
459 similar arcuate fractures at Midtre Lovénbreen as englacial thrust planes.
460 Nonetheless, it is hard to envisage that all of the reflectors in the GPR profiles

represent englacial thrusts. Other studies have identified debris-rich englacial thrusts with GPR at a number of other glaciers in the region, including Scott Turnerbeen (Sletten et al., 2001), Bakaninbreen (Murray et al., 1997) and nearby Kongsvegen (Murray and Booth, 2010). Radar images of dipping reflectors from Austre Lovénbreen appear distinct from englacial thrust reflectors reported at Kongsvegen by Murray and Booth (2010) which, at Kongsvegen, appear to be isolated, discrete and thicker features than are found at Austre Lovénbreen.

A further possibility is that the dipping structures within the moraine represent layering within buried basal ice. Debris-laden basal ice commonly has a layered appearance derived either from freeze-on of packages of water and sediment to the glacier base, or from regelation, and may have a sediment content from 0 to ~90% (e.g. Hubbard and Sharp, 1989; Knight, 1997; Hubbard et al., 2009). Further, the folding in the layers is also consistent with reports of tectonic deformation within basal ice layers (e.g. Waller et al., 2000), perhaps in this case caused by compression against the adverse bed slope, or the cold-based margin, or possibly during a surge event. Several processes could contribute to basal ice formation at Austre Lovénbreen including regelation as the glacier slides over bedrock in the temperate zone up-glacier from the terminus (e.g. Hubbard and Sharp, 1993), and seasonal freeze-on of meltwater and sediment at the glacier terminus (e.g. Weertman, 1961). Additionally, analysis of the GPR profile of Saintenoy et al. (2013) demonstrates that the adverse bed slope of the basin beneath Austre Lovénbreen is ~1.6 times steeper than the ice surface slope. Hence, the bed slope meets the threshold necessary to permit the operation of glaciohydraulic

supercooling and associated freeze-on of water and sediment (e.g. Lawson et al., 1998; Cook et al., 2010). There are no reports, however, of any field evidence diagnostic of the operation of supercooling (cf. Evenson et al., 1999; Cook et al., 2006). Regelation is unlikely to produce the thick sequences of ice and sediment shown in the GPR profiles, as basal ice thicknesses associated with regelation are generally less than ~1m due to ice melting from the base during glacier sliding (e.g. Hubbard and Sharp, 1989; Knight, 1997). Basal ice could be formed by freeze-on, either seasonally or possibly through supercooling. Our favoured hypothesis is that post-formational flow-related deformation in the form of strong longitudinal compression has led to the stacking of the debris-rich layers (e.g. Waller et al., 2000). Strong longitudinal compression could be caused by either: (1) the subglacial overdeepening (based on our interpretation of the GPR profiles undertaken by Saintenoy et al., 2013); (2) the glacier margin during the Neoglacial maximum; or (3) associated with a surge.

The buried basal ice could be composed of a range of descriptively different facies, possibly with different origins. However, at the resolution of the radar imagery the most appropriate classification is banded basal ice (i.e. layering on the scale of centimetres to decimetres), according to the classification scheme of Hubbard et al. (2009). Care must be taken with the interpretation of the reflector angle of dip as the survey lines may not run parallel to the direction of dip of the reflectors in each case. What is recorded, therefore, is an apparent dip, rather than an actual dip. Further work involving three-dimensional GPR profiling of the reflectors could resolve this issue.

511 *6.5. Landform stability and preservation potential*

512 Despite its high ice content, the moraine within zones A–C appears relatively
513 stable. Examination of aerial imagery reveals an absence of slope failure and
514 back wasting features (Fig. 2) that are characteristic of moraines with high
515 rates of ablation of incorporated buried ice (e.g. Bennett et al., 2000). It is,
516 however, likely that surface lowering is occurring, as repeat lidar surveys of
517 the north east side of the outer complex at the adjacent Midtre Lovénbreen has
518 shown surface lowering of 0.65 m a^{-1} (±0.2 m) (Irvine-Fynn et al., 2011).
519 Schomaker and Kjær (2008) also recognised similar downwasting rates of
520 0.9 m a^{-1} from 1983 to 2004 at Holmströmbreen in central Spitsbergen. Given
521 the mean summer temperature of 3.8 °C recorded during the 1981-2010
522 period at nearby Ny-Ålesund (Førland et al., 2011), it is likely that the buried
523 ice at Austre Lovénbreen experiences some ablation during the summer
524 months. So zones A–C of the outer moraine complex are downwasting, rather
525 than backwasting. The dampening effect on ablation of the thin protective
526 surface debris layer will depend upon: (1) the thickness of the debris layer; (2)
527 the thermal conductivity of the debris type; and (3) the water content of the
528 surface debris layer (Schomacker, 2008). Other potential factors that result in
529 a difference between the stability of the surface debris layer of the ice-cored
530 lateral moraines at Austre Lovénbreen and nearby Kongsvegen (outlined by
531 Bennett et al., 2000) include a potentially thicker surface debris layer and/or
532 coarser surface debris that promote drainage. A freely drained surface debris
533 layer would be less prone to slope failure and exposure of the underlying ice,
534 but would have a higher thermal conductivity, so could act to either promote

535 or inhibit the ablation of the buried ice. Rates of dead-ice ablation can be
536 similar in both the cold arid Svalbard climate and the mild humid climate of
537 Iceland (Schomaker and Kjær, 2008). This outer moraine complex at Austre
538 Lovénbreen is located away from the proglacial fluvial discharge routes of both
539 Austre and Midtre Lovénbreen: this is likely to be the key issue facilitating the
540 lack of backwasting and apparent stability of the landform.

541 The moraine within zone D contains a relatively small amount of ice and the
542 porosity of the debris is, therefore, important to understand how the
543 incorporated ice influences its morphology. Whilst Kilfeather and van der Meer
544 (2008) note that 'till porosity has largely been ignored', a range of likely
545 porosity values can be assessed (Table 6). The Austre Lovénbreen outer
546 moraine is likely to have a porosity value of between 0.15 and 0.30, based
547 upon comparison to other similar sedimentary and morphological settings. The
548 outer moraine within zone D at Austre Lovénbreen is, therefore, likely to
549 experience little modification associated with the removal of 20–40%
550 interstitial ice. High preservation potential of the outer moraine morphology in
551 zone D is, therefore, likely to occur even following the complete ablation of the
552 incorporated ice.

553

554 **7. Conclusions**

555 1. Buried ice forms the dominant component of the Austre Lovénbreen
556 outer moraine in the upper lateral zone, whereas sediment forms the
557 dominant component of the frontal zone.

2. Many examples of ice forming unstable components of landforms have been recognised and are associated with sediment reworking, but this example at Austre Lovénbreen illustrates that ice can, so far, form a relatively stable component of landforms without sediment reworking, although landform degradation will still occur.
3. The rate of surface lowering associated with ablation of buried ice is likely to have increased associated with the local change from a summer temperature of 3.4 °C (1961–1990) to 3.8 °C (1981–2010). This ablation rate is likely to increase further if local air temperature also increases.
4. Because of the ice-debris mix within the outer moraine, following complete climatic amelioration, the preservation potential of any geomorphological feature associated with the upper lateral moraine (zones A–B) is negligible. The preservation potential of the frontal moraine, however, is high, with little change predicted in the contemporary geomorphology resulting from the complete meltout of the interstitial ice component that is currently preserved by the low temperature and lack of ice exposure by surface sediment reworking.
5. The ice within the lateral-frontal moraine is likely to be composed of basal ice derived from freeze-on of ice and sediment to the glacier bed. Post-formational deformation, in the form of strong longitudinal compression, has subsequently led to a stacking and thickening of the sequence.
6. The glacier surface bulge identified on the 1936 aerial imagery provides evidence that Austre Lovénbreen has previously displayed surge activity,

583 although given the current state of the thermal regime and recent mass
584 balance it is highly unlikely to do so in the near future.
585 7. This research shows the value of relict buried ice that is preserved in
586 landforms to aiding our understanding of former glacier characteristics.
587 8. Further research on the stable isotope composition, sedimentology of
588 included debris, and crystallography of the buried ice at Austre
589 Lovénbreen will aid our understanding of both its origin and its value as
590 an archive of palaeoglaciological information from the Neoglacial.

591

592 **Acknowledgements**

593 The research was funded by grants from Nottingham Trent University (to NGM)
594 and the Royal Society (2007/R2 to DJG/NGM). The fieldwork benefited from
595 the logistical support provided by Steinar Aksnes of the Norwegian Polar
596 Institute's Sverdrup Station. Tris Irvine-Fynn is thanked for the provision of
597 height data for a number of positions outside of the moraine-mound complex.
598 This manuscript benefitted from reviews and editorial comment by three
599 anonymous reviewers and Richard Marston.

600

References

Bennett, M.R., Huddart, D., Glasser, N.F., Hambrey, M.J., 2000. Resedimentation of debris on an ice-cored lateral moraine in the high-Arctic (Kongsvegen, Svalbard). Geomorphology 35 (1–2), 21–40.

Boulton, G.S., Eyles, N., 1979. Sedimentation by valley glaciers: a model and genetic classification. In: Schluchter, C. (Ed.), Moraines and Varves. Balkema, Rotterdam, pp. 11–23.

Burki, V., Hansen, L., Fredin, O., Andersen, T.A., Beylich, A.A., Jaboyedoff, M., Larsen, E., Tønnesen, J.-F. 2010. Little Ice Age advance and retreat sediment budgets for an outlet glacier in western Norway. Boreas 39 (3), 551–566.

Cook, S.J., Waller, R.I., Knight, P.G., 2006. Glaciohydraulic supercooling: the process and its significance. Progress in Physical Geography 30 (5), 577-588.

Cook S.J., Robinson Z.P., Fairchild, I.J., Knight, P.G., Waller, R.I., Boomer, I., 2010. Role of glaciohydraulic supercooling in the formation of stratified facies basal ice: Svínafellsjökull and Skaftafellsjökull, southeast Iceland. Boreas 39 (1), 24–38.

Cook, S.J., Graham, D.J., Swift, D.A., Midgley, N.G., Adam, W.G., 2011. Sedimentary signatures of basal ice formation and their preservation within ice-marginal sediments. Geomorphology 125 (1), 122–131.

Embleton, C., King, C.A., 1975. Glacial and Periglacial Geomorphology, Arnold, London.

622 Etzelmüller, B., Ødegård, R.S., Vatne, G., Mysterud, R.S., Tonning, T., Sollid,
623 J.L., 2000. Glacier characteristics and sediment transfer system of
624 Longyearbreen and Larsbreen, western Spitsbergen. Norsk Geografisk
625 Tidsskrift 54 (4), 157–168.

626 Evans, D.J.A., 2009. Controlled moraines: origins, characteristics and
627 palaeoglaciological implications. Quaternary Science Reviews 28 (3–4), 183–
628 208.

629 Evenson, E.B., Lawson, D.E., Strasser, J.C., Larson, G.J., Alley, R.B.,
630 Ensminger, S.L., Stevenson, W.E., 1999. Field evidence for the recognition of
631 glaciohydraulic supercooling. In: Mickelson, D.M., Attig, J.W. (Eds.), Glacial
632 Processes: Past and Present. Geological Society of America, Special Paper 337,
633 pp. 23–35.

634 Ewertowski M., Kasprzak L., Szuman I., Tomczyk A.M., 2012. Controlled, ice-
635 cored moraines: sediments and geomorphology. An example from
636 Ragnarbreen, Svalbard. Zeitschrift für Geomorphologie 51 (1), 53–74.

637 Flint, R.F., 1971. Glacial and Quaternary geology. John Wiley and Sons, New
638 York.

639 Førland, E.J., Benestad, R., Hanssen-Bauer, I., Haugen, J.E., Skaugen, T.E.,
640 2011. Temperature and precipitation development at Svalbard 1900–2100.
641 Advances in Meteorology, 893790.

642 Friedt, J-M., Tolle, F., Bernard, É., Griselin, M., Laffly, D., Marlin, C., 2012.
643 Assessing the relevance of digital elevation models to evaluate glacier mass

644 balance: application to Austre Lovénbreen (Spitsbergen, 79°N). Polar Record
645 48 (244), 2–10.

646 Glasser, N.F., Hambrey, M.J., 2003. Ice-marginal terrestrial landsystems:
647 Svalbard polythermal glaciers. In: Evans, D.J.A. (Ed.) Glacial Landsystems.
648 Hodder Arnold, London, pp. 65–88.

649 Graham, D.J., 2002. Moraine-mound formation during the Younger Dryas in
650 Britain and the Neoglacial in Svalbard. PhD thesis, University of Wales,
651 Aberystwyth, UK.

652 Hagen, J.O., Leistøl, O., Roland, E., Jørgensen, T., 1993. Glacier atlas of
653 Svalbard and Jan Mayen. Norsk Polarinstitutt, Meddelelser.

654 Hamberg, A., 1984. En resa till norra Ishafvet sommaren 1892. Ymer 14, 25–
655 61.

656 Hambrey, M.J., Glasser, N.F., 2003. The role of folding and foliation
657 development in the genesis of medial moraines: examples from Svalbard
658 glaciers. Journal of Geology 111 (4), 471–485.

659 Hambrey, M.J., Bennett, M.R., Dowdeswell, J.A., Glasser, N.F., Huddart, D.,
660 1999. Debris entrainment and transfer in polythermal valley glaciers. Journal
661 of Glaciology 45 (149), 69–86.

662 Hambrey, M.J., Murray, T., Glasser, N.F., Hubbard, A., Hubbard, B., Stuart, G.,
663 Hansen, S., Kohler, J., 2005. Structure and changing dynamics of a
664 polythermal valley glacier on a centennial time-scale: midre Lovénbreen,
665 Svalbard. Journal of Geophysical Research, Earth Surface F010006.

666 Hansen, S., 2003. From surge-type to non-surge type glacier behaviour: Midre
667 Lovénbreen, Svalbard. Annals of Glaciology 36, 97–102.

668 Hodgkins, R., Hagen, J.O., Hamran, S.-E., 1999. Twentieth-century mass
669 balance and thermal regime change at an Arctic glacier. Annals of Glaciology
670 28, 216–220.

671 Hubbard, B., Sharp, M.J., 1989. Basal ice formation and deformation: a review.
672 Progress in Physical Geography 13 (4), 529–558.

673 Hubbard, B., Sharp, M.J., 1993. Weertman regelation, multiple refreezing
674 events and the isotopic evolution of the basal ice layer. Journal of Glaciology
675 39 (132), 275–291.

676 Hubbard, B., Cook, S., Coulson, H., 2009. Basal ice facies: a review and
677 unifying approach. Quaternary Science Reviews 28 (19–20), 1956–1969.

678 Humlum, O., Elberling, B., Hormes, A., Fjordheim, K., Hansen, O.H. and
679 Heinemeier, J., 2005. Late-Holocene glacier growth in Svalbard, documented
680 by subglacial relict vegetation and living soil microbes. The Holocene 15 (3),
681 396–407.

682 IPCC, 2007. Climate Change 2007: The physical science basis. Contribution of
683 working group I to the fourth assessment report of the Intergovernmental
684 Panel on Climate Change. Solomon, S., Qin, D., Manning, M., Chen, Z.,
685 Marquis, M., Averyt, K.B., Tignor, M.M.B., Miller, H.L. (Eds.). Cambridge
686 University Press, Cambridge, UK and New York, NY, USA, pp. 996.

687 Irvine-Fynn, T.D.L., Barrand, N.E., Porter, P.R., Hodson, A.J., Murray, T., 2011.
688 Recent High-Arctic glacial sediment redistribution: A process perspective using
689 airborne lidar. Geomorphology 125 (1), 27–39.

690 Jiskoot, H., Murray, T., Boyle, P.J., 2000. Controls on the distribution of surge-
691 type glaciers in Svalbard. Journal of Glaciology 46 (154), 412–422.

692 Kilfeather, A.A., van der Meer, J.J.M., 2008. Pore size, shape and connectivity
693 in tills and their relationship to deformation processes. Quaternary Science
694 Reviews 27 (3–4), 250–266.

695 Knight, P.G., 1997. The basal ice layer of glaciers and ice sheets. Quaternary
696 Science Reviews 16 (9), 975–993.

697 Knight, P.G., Patterson, C.J., Waller, R.I., Jones, A.P., Robinson, Z.P., 2000.
698 Preservation of basal-ice sediment texture in ice sheet moraines. Quaternary
699 Science Reviews 19 (13), 1255–1258.

700 Lawson, D.E., 1979. Sedimentological analysis of the western terminus region
701 of the Matanuska Glacier, Alaska. Cold Regions Research and Engineering
702 Laboratory Report 79–9, pp. 112.

703 Lawson, D.E., Strasser, J.C., Evenson, E.B., Alley, R.B., Larson, G.J., Arcone,
704 S.A., 1998. Glaciohydraulic supercooling: a freeze-on mechanism to create
705 stratified, debris-rich basal ice: I. Field Evidence. Journal of Glaciology 44
706 (148), 547–562.

707 Liestøl, O. 1988. The glaciers in the Kongsfjorden area, Svalbard. Norsk
708 Geografisk Tidsskrift 42 (4), 231–238.

709 Lønne, I., 2007. Reply to Lukas, S., Nicholson, L.I., Humlum, O. (2006).
710 Comment on Lønne and Lysså (2005): Deglaciation dynamics following the
711 Little Ice Age on Svalbard: Implications for shaping of landscapes at high
712 latitudes. Geomorphology 72, 300–319. Geomorphology, 86 (1–2), 217–218.

713 Lønne, I., Lauritsen, T., 1996. The architecture of a modern push-moraine at
714 Svalbard as inferred from ground-penetrating radar. Arctic and Alpine
715 Research 28 (4), 488–495.

716 Lønne, I. and Lysså, A., 2005. Deglaciation dynamics following the Little Ice Age
717 on Svalbard: implications for shaping of landscapes at high latitudes.
718 Geomorphology 72 (1–4), 300–319.

719 Lukas, S., Nicholson, L.I., Ross, F.H., Humlum, O., 2005. Formation, meltout
720 processes and landscape alteration of High-Arctic ice-cored moraines –
721 examples from Nordenskiold Land, Central Spitsbergen. Polar Geography 29
722 (3), 157–187.

723 Lukas, S., Nicholson, L.I., Humlum, O., 2007. Comment on Lønne and Lysså
724 (2005): “Deglaciation dynamics following the Little Ice Age on Svalbard:
725 Implications for shaping of landscapes at high latitudes”, Geomorphology 72,
726 300–319. Geomorphology 84 (1–2), 145–149.

727 Lysså, A., Lønne, I., 2001. Moraine development at a small High-Arctic valley
728 glacier: Rieperbreen, Svalbard. Journal of Quaternary Science 16 (6), 519–529.

729 Midgley, N.G., Glasser, N.F., Hambrey, M.J., 2007. Sedimentology, structural
730 characteristics and morphology of a Neoglacial high-Arctic moraine-mound
731 complex: Midre Lovénbreen, Svalbard. In: Hambrey, M.J., Christoffersen, P.,

732 Glasser, N.F., Hubbard, B. (Eds.), Glacial Sedimentary Processes and Products,
733 International Associated of Sedimentologists, Special Publication 39, pp. 11–23.

734 Murray, T., Booth, A.D., 2010. Imaging glacial sediment inclusions in 3-D using
735 ground-penetrating radar at Kongsvegen, Svalbard. Journal of Quaternary
736 Science 25 (5), 754–761.

737 Murray, T., Gooch, D.L., Stuart, G.W., 1997. Structures within the surge front
738 at Bakaninbreen, Svalbard, using ground-penetrating radar. Annals of
739 Glaciology 24, 122–129.

740 Parriaux, A., Nicoud, G.F., 1990. Hydrological behaviour of glacial deposits in
741 mountainous areas. In: Molnár, L. (Ed.), Hydrology of Mountainous Areas.
742 International Association of Hydrological Sciences, Publication 190, pp. 291–
743 311.

744 Reynolds, J. 2011. An Introduction to Applied and Environmental Geophysics.
745 John Wiley and Sons, Chichester.

746 Rippin, D., Willis, I., Kohler, J., 2007. Changes in the thermal regime of the
747 polythermal Midre Lovénbreen, Svalbard. Geophysical Research Abstracts 9,
748 03737.

749 Ronnert, L., Mickelson, D.M., 1992. High porosity of basal till at Burroughs
750 Glacier, southeastern Alaska. Geology 20 (9), 849–852.

751 Saintenoy, A., Friedt, J.-M., Booth, A.D., Tolle, F., Bernard, E., Laffly, D.,
752 Marlin C., Griselin, M., 2013. Deriving ice thickness, glacier volume and

753 bedrock morphology of Austre Lovénbreen (Svalbard) using GPR. Near Surface
754 Geophysics 11 (2), 253–261.

755 Schomacker, A., 2008. What controls dead-ice melting under different climate
756 conditions? A discussion. Earth-Science Reviews 90 (3–4), 103–113.

757 Schomaker, A., Kjær, K.H., 2008. Quantification of dead-ice melting in ice-
758 cored moraines at the high-Arctic glacier Holströmbreen, Svalbard. Boreas 37
759 (2), 211–225.

760 Schwamborn, G., Heinzel, J., Schirrmeister, L., 2008. Internal characteristics
761 of ice-marginal sediments deduced from georadar profiling and sediment
762 properties (Brøgger Peninsula, Svalbard). Geomorphology 95 (1–2), 74–83.

763 Sharp M.J., Jouzel, J., Hubbard, B., Lawson, W., 1994. The character, structure
764 and origin of the basal ice layer of a surge-type glacier. Journal of Glaciology
765 40 (135), 327–340.

766 Sletten, K., Lysså, A., Lønne, I., 2001. Formation and disintegration of a high-
767 arctic ice-cored moraine complex, Scott Turnerbreen, Svalbard. Boreas 30 (4),
768 272–284.

769 Sugden. D.E., John, B.S., 1976. Glaciers and Landscape: A Geomorphological
770 Approach. Edward Arnold, London.

771 Swift, D.A., Evans, D.J.A., Fallick, A.E., 2006. Transverse englacial debris-rich
772 ice bands at Kvíárjökull, southeast Iceland. Quaternary Science Reviews 25
773 (13–14), 1708–1718.

774 Svendsen, J.-I., Mangerud, J., 1997. Holocene glacial and climatic variations
775 on Spitsbergen, Svalbard. The Holocene 7 (1), 45–57.

776 Waller, R.I., Hart, J.K., Knight, P.G., 2000. The influence of tectonic
777 deformation on facies variability in stratified debris-rich basal ice. Quaternary
778 Science Reviews 19 (8), 775–786.

779 Weertman, J., 1961. Mechanism for the formation of inner moraines found
780 near the edge of cold ice caps and ice sheets. Journal of Glaciology 3 (30),
781 965–978.

782 WGMS (2011). Glacier Mass Balance Bulletin No. 11 (2008–2009). Zemp, M.,
783 Nussbaumer, S.U., GärtnerRoer, I., Hoelzle, M., Paul, F., Haeberli, W. (Eds.),
784 ICSU(WDS)/IUGG(IACS)/UNEP/UNESCO/WMO, World Glacier Monitoring
785 Service, Zurich, Switzerland, pp. 102.

786 Worni, R., Stoffel, M., Huggel, C., Volz, C., Casteller, A., Luckman, B., 2012.
787 Analysis and dynamic modeling of a moraine failure and glacier lake outburst
788 flood at Ventisquero Negro, Patagonian Andes (Argentina). Journal of
789 Hydrology 444–445, 134–145.

790

791 **Table 1** Common mid-point (CMP) survey velocities obtained for each ground-
792 penetrating radar (GPR) transect at Austre Lovénbreen (multiple values
793 indicate velocities obtained from different CMP surveys undertaken along each
794 transect).

Transect	CMP velocity (m ns^{-1})
1	0.17
2	0.16 & 0.17
3	0.16
4	0.17
5	0.17, 0.16, 0.16, 0.17 & 0.17
6	0.15 & 0.15
7	0.15
8	0.14
9	0.14, 0.14 & 0.13

795

Table 2 Summary table of radar facies in the Austre Lovénbreen outer lateral-frontal moraine.

Transect	Relative velocity	Signal attenuation	Dipping reflectors	Syncline structure	Surface parallel reflectors	Hyperbolae	Debris component	Ice component	Zone
1	high	low	common	vague	absent	common	limited	dominant	A
2	high	low	abundant	not found	absent	scarce	limited	dominant	B
3	high	low	abundant	vague	absent	scarce	limited	dominant	B
4	high	low	abundant	vague	absent	scarce	limited	dominant	B
5	high	low	abundant	vague	absent	scarce	limited	dominant	B
6	moderate	moderate	abundant	clear	absent	moderate	ice-debris mix	ice-debris mix	C
7	moderate	high	scarce	absent	present	ubiquitous	ice-debris mix	ice-debris mix	C
8	low	high	scarce	absent	present	ubiquitous	dominant	limited	D
9	low	high	scarce	absent	present	ubiquitous	dominant	limited	D

798 **Table 3** Relative abundance of reflector apparent angle of dip at the moraine
799 surface.

Transect	Apparent angle of dip				
	10°	11-20°	21-30°	31-40°	41-50°
1		•••••	•		
2					••••••
3			•	•	• •••
4				•	• ••••
5				•	• ••••
6			•	••	•••
7	•	••	•••		
8			•	••••	•
9	•	•	•••	•	

800

801

802 **Table 4** Common radar velocities (as cited by Schwamborn et al., 2008;
803 Murray and Booth 2010; Reynolds, 2011).

Material	Radar velocity (m ns^{-1})
air	0.3
snow	0.194-0.252
glacier ice	0.168-0.172
permafrost consisting of clast-rich intermediate diamicton with 10% interstitial ice	0.127
water (fresh)	0.033

804

805

806 **Table 5** Known radar velocities and interpreted velocities of ice-debris mixes.

Radar velocity (m ns^{-1})	substrate ice component	substrate debris component	interpreted substrate ice component	interpreted substrate debris component
0.17 [a]	100%	0%		
0.16			80%	20%
0.15			60%	40%
0.14			40%	60%
0.13			20%	80%
0.127 [b]	10%	90%		

807 [a] commonly accepted value for glacier ice (e.g. Saintenoy et al., 2013)

808 [b] velocity value for diamicton with 10% interstitial ice found by Schwamborn et
809 al. (2008) at the adjacent Midtre Lovénbreen

810

811 **Table 6** Example porosities associated with a range of glacial sediments and landforms.

Debris / landform type	Porosity	Source
Pleistocene till samples	0.01-0.19	Kilfeather and van der Meer, 2008
lateral moraine	0.10-0.15	Parriaux and Nicoud, 1990
value used to model terminal moraine failure and associated glacial lake outburst flood	0.15	Worni et al., 2012
frontal moraine	0.15-0.25	Parriaux and Nicoud, 1990
supraglacial till	0.20-0.40	Parriaux and Nicoud, 1990
B0dalen valley diamictons	0.25-0.40	Burki et al., 2010
recently deposited till from debris-rich basal ice	0.26-0.39	Ronnert and Mickelson, 1992
recently deposited diamicton at Matanuska glacier	0.30-0.50	Lawson, 1979

812

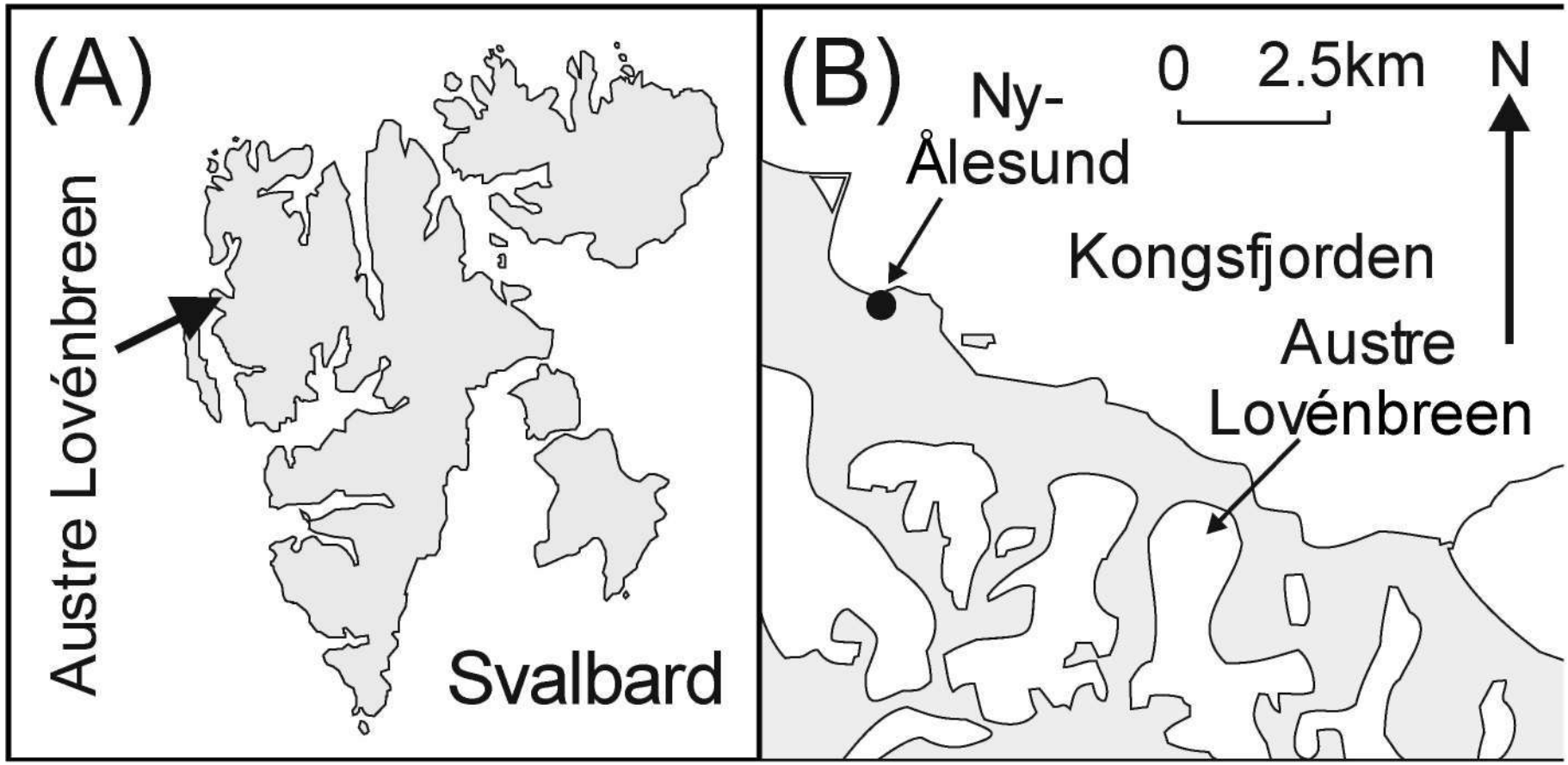

Figure 1 Location of: (A) Austre Lovénbreen on Svalbard in the Norwegian high-Arctic; (B) Austre Lovénbreen on Brøggerhalvøya near Ny-Ålesund.

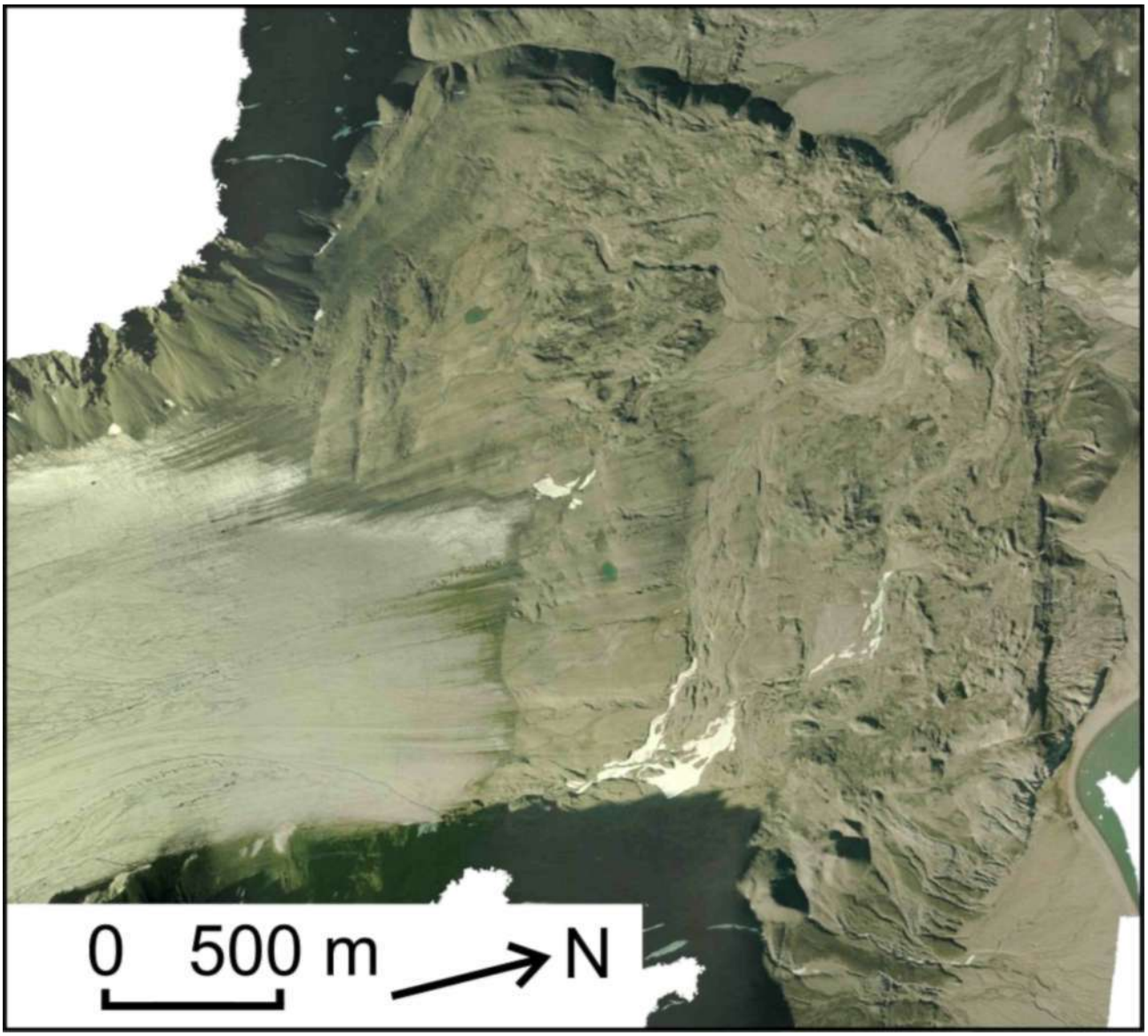

Figure 2 (A) Aerial image of the terminus of Austre Lovénbreen (summer 2003) and the proglacial area; (B) outline of the Neoglacial lateral-frontal moraine and the location of the GPR transects. Aerial image data from the UK Natural Environment Research Council (NERC) Airborne Research and Survey Facility (ARSF) are provided courtesy of NERC via the NERC Earth Observation Data Centre (NEODC).

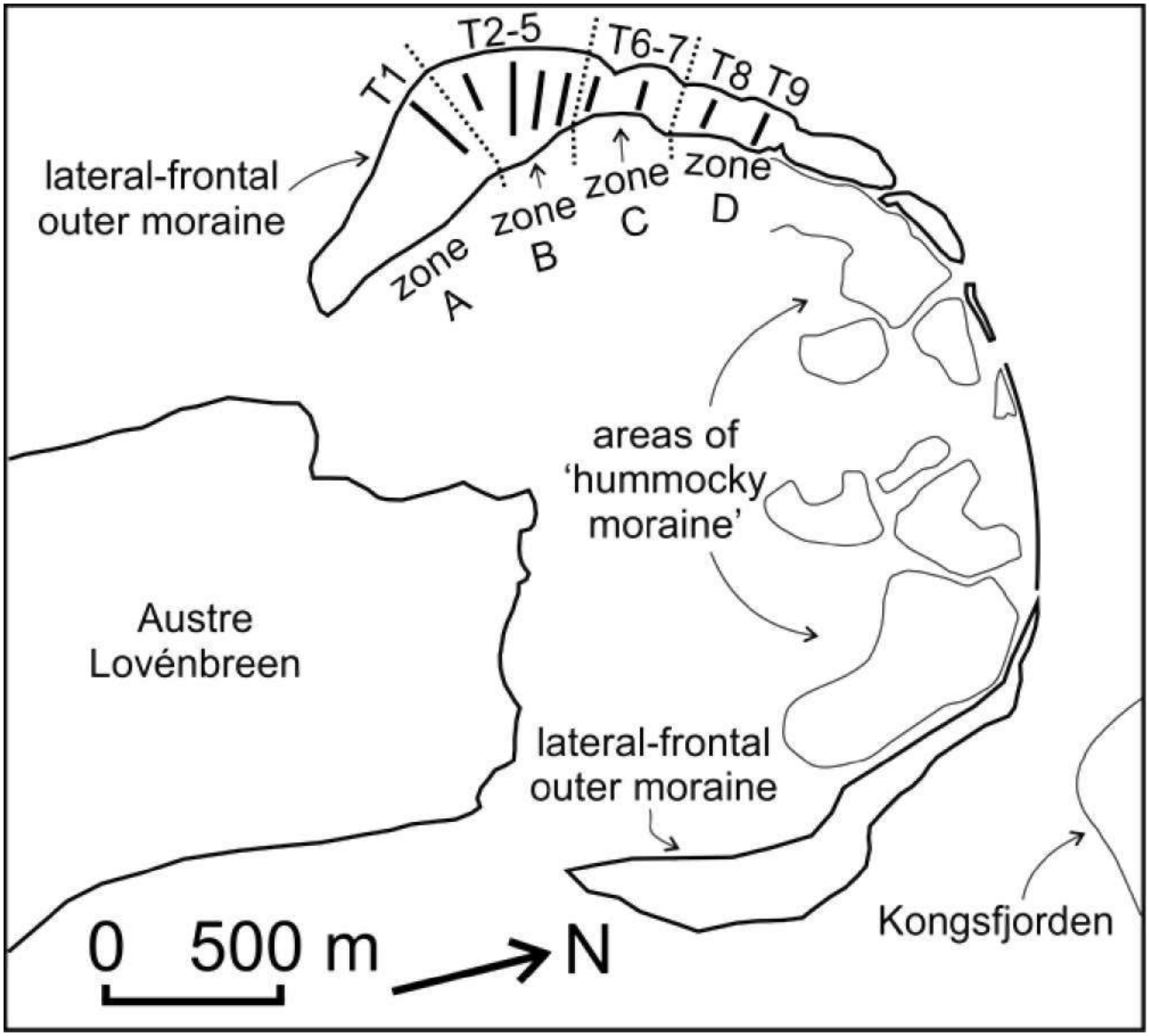

Figure 2 (A) Aerial image of the terminus of Austre Lovénbreen (summer 2003) and the proglacial area; (B) outline of the Neoglacial lateral-frontal moraine and the location of the GPR transects. Aerial image data from the UK Natural Environment Research Council (NERC) Airborne Research and Survey Facility (ARSF) are provided courtesy of NERC via the NERC Earth Observation Data Centre (NEODC).

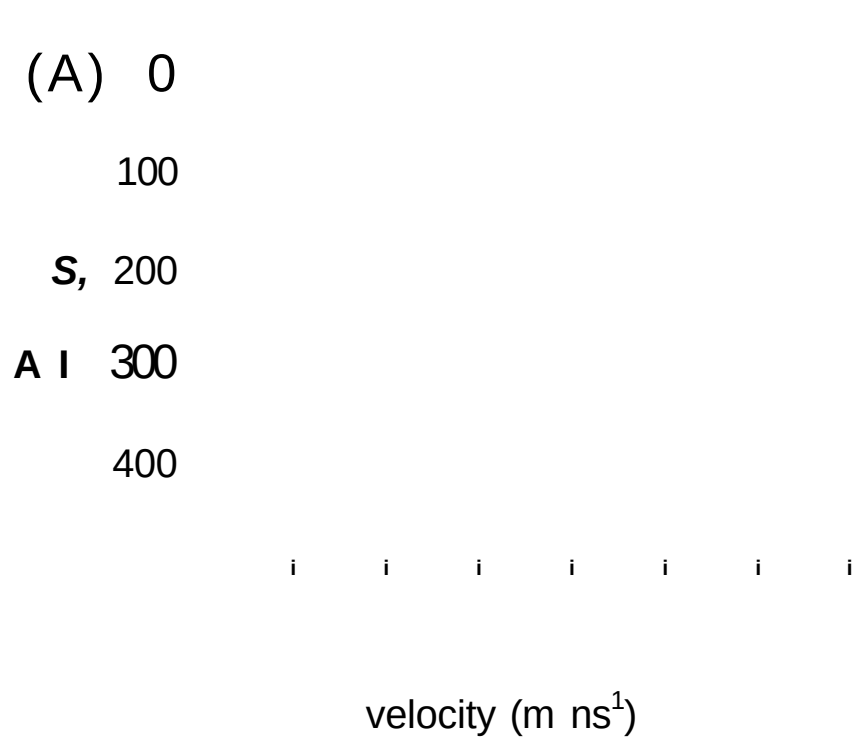

Figure 3 (A) Example common mid-point (CMP) survey across transect 2; (B) CMP survey across transect 9.

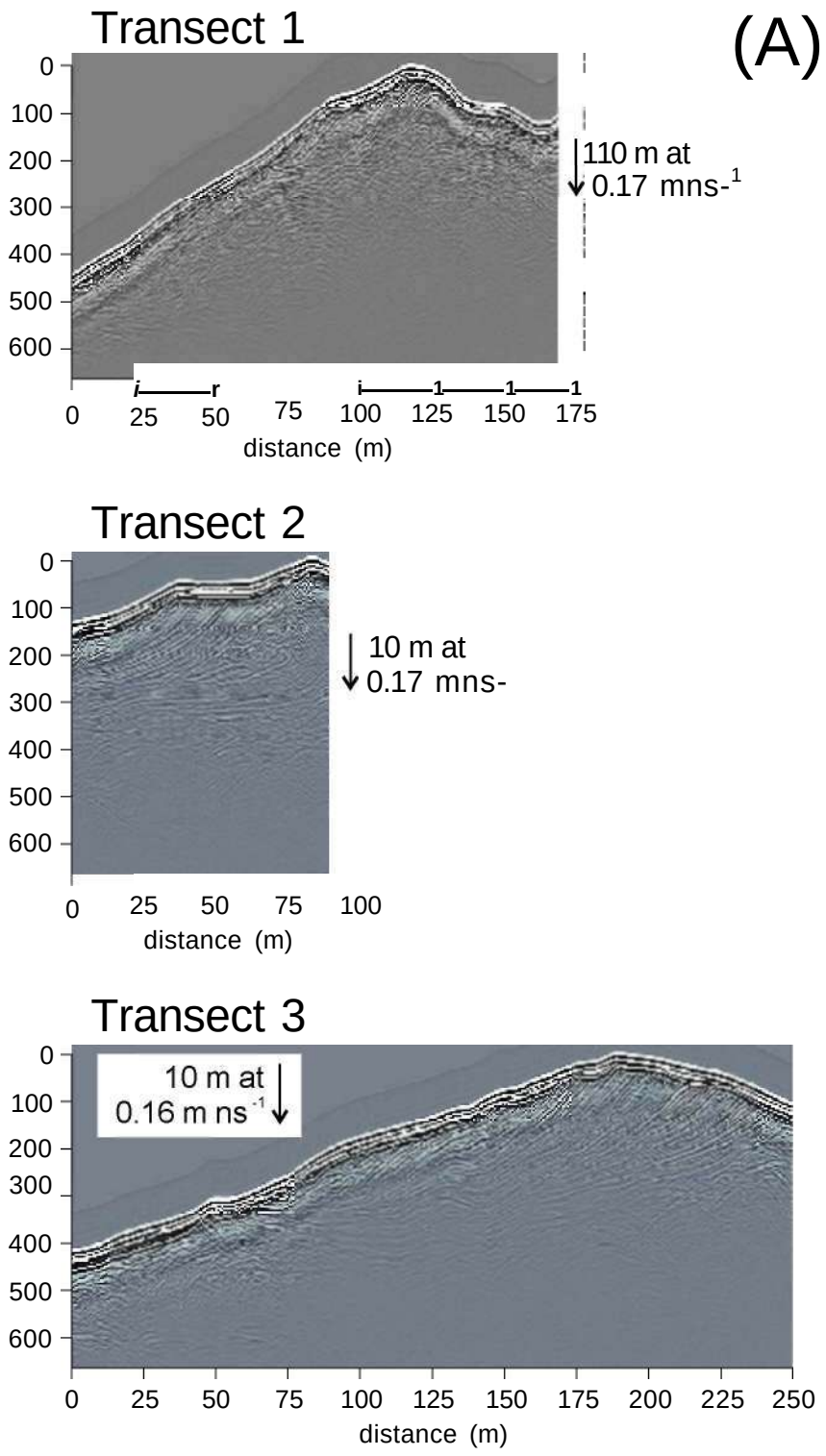

Figure 4 Ground-penetrating radar (GPR) surveys as grey-scale images: (A) transects 1–3; (B) transects 4–6; and (C) transects 7–9.

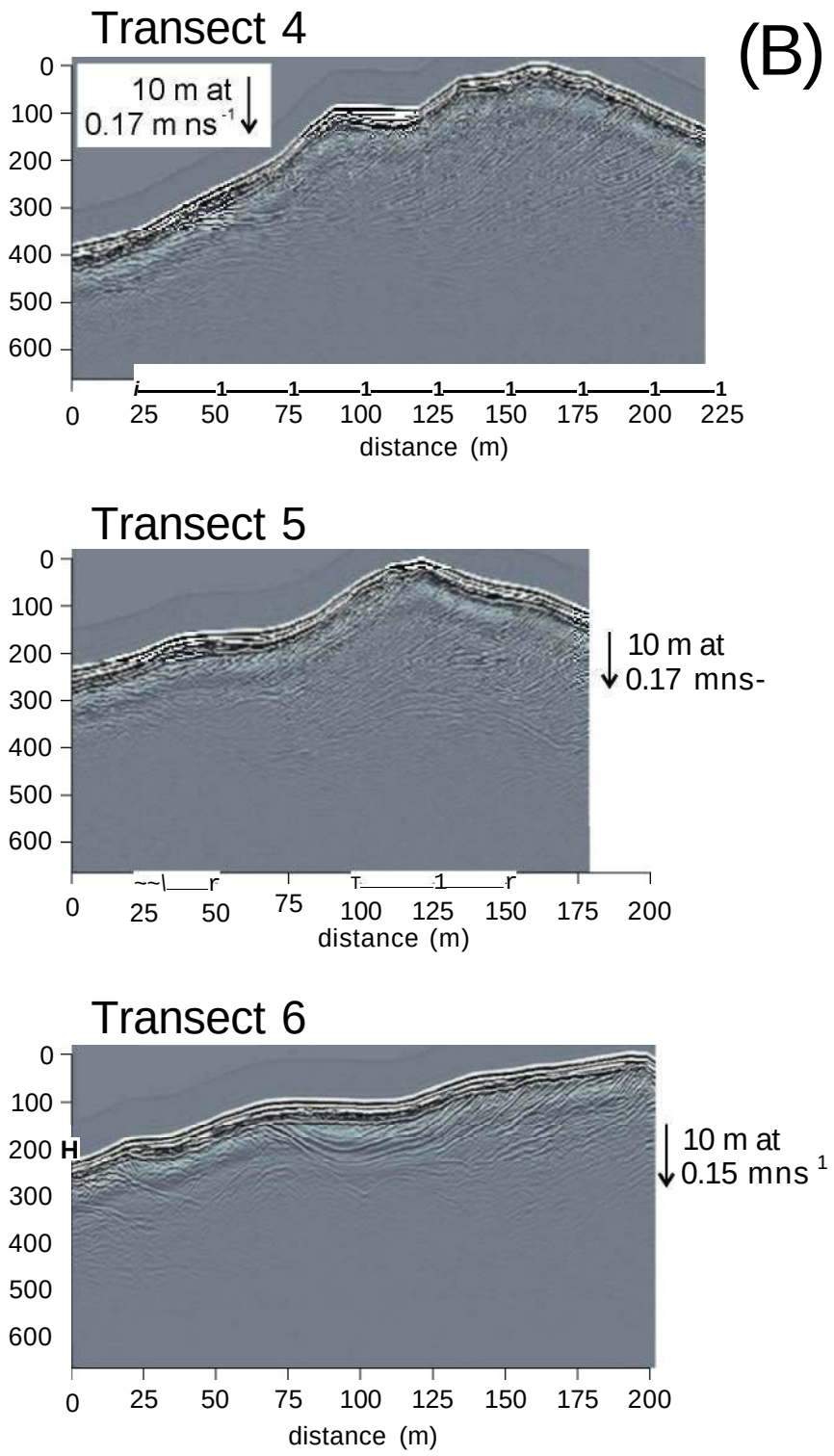

Figure 4 Ground-penetrating radar (GPR) surveys as grey-scale images: (A) transects 1–3; (B) transects 4–6; and (C) transects 7–9.

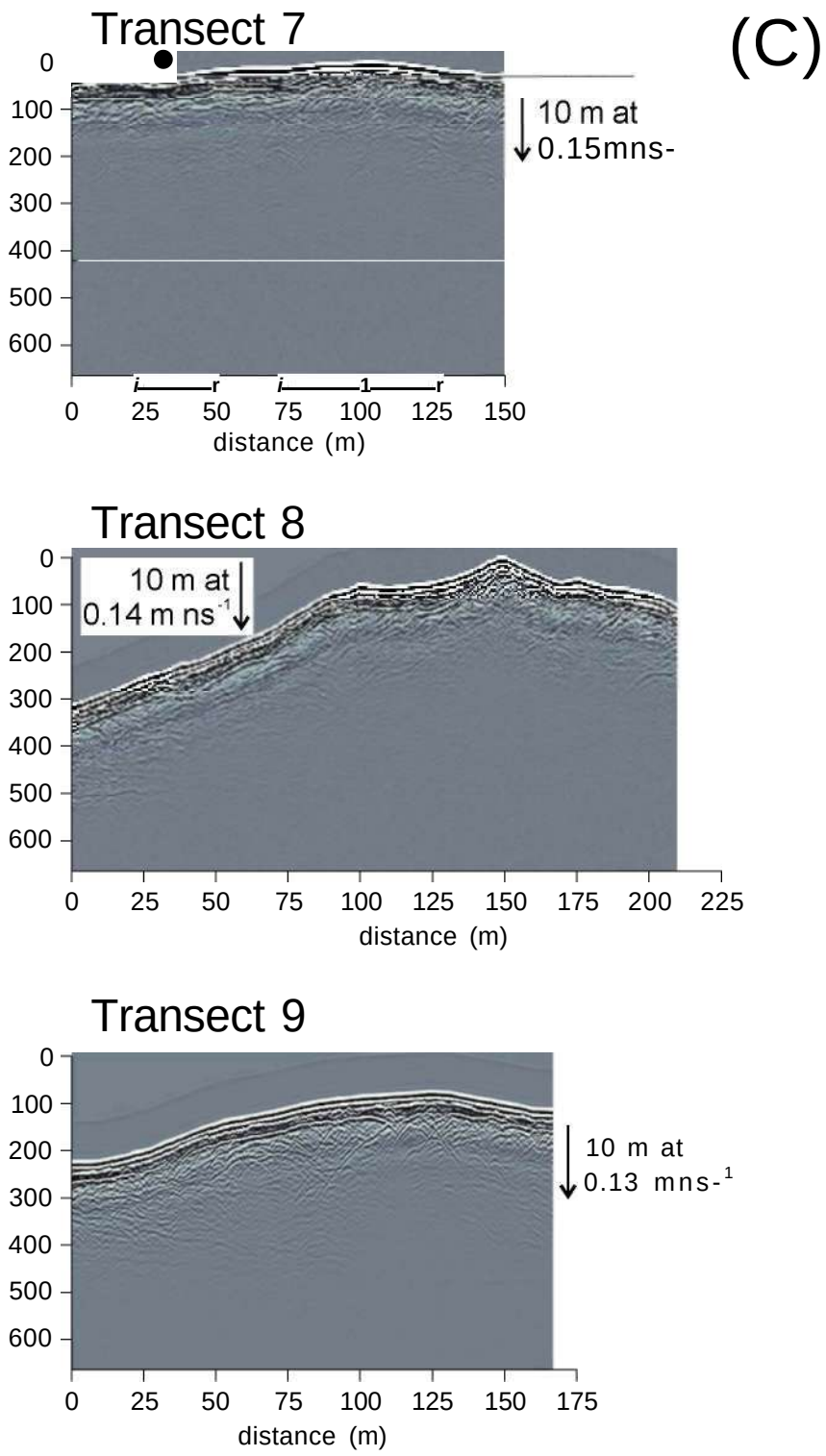

Figure 4 Ground-penetrating radar (GPR) surveys as grey-scale images: (A) transects 1–3; (B) transects 4–6; and (C) transects 7–9.

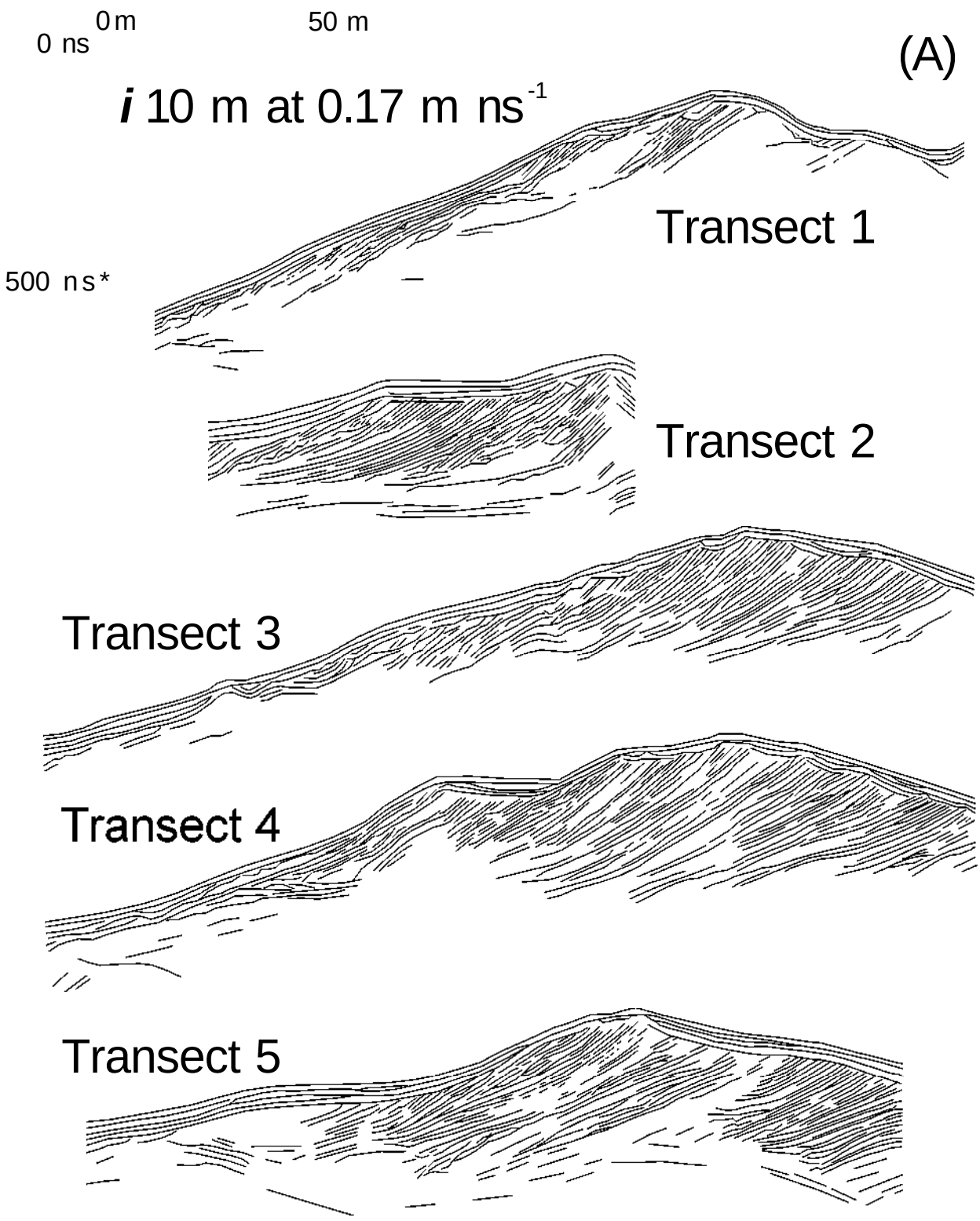

Figure 5 Key reflection characteristics of ground-penetrating radar (GPR) surveys from transects 1–5 (A) and transects 6–9 (B).

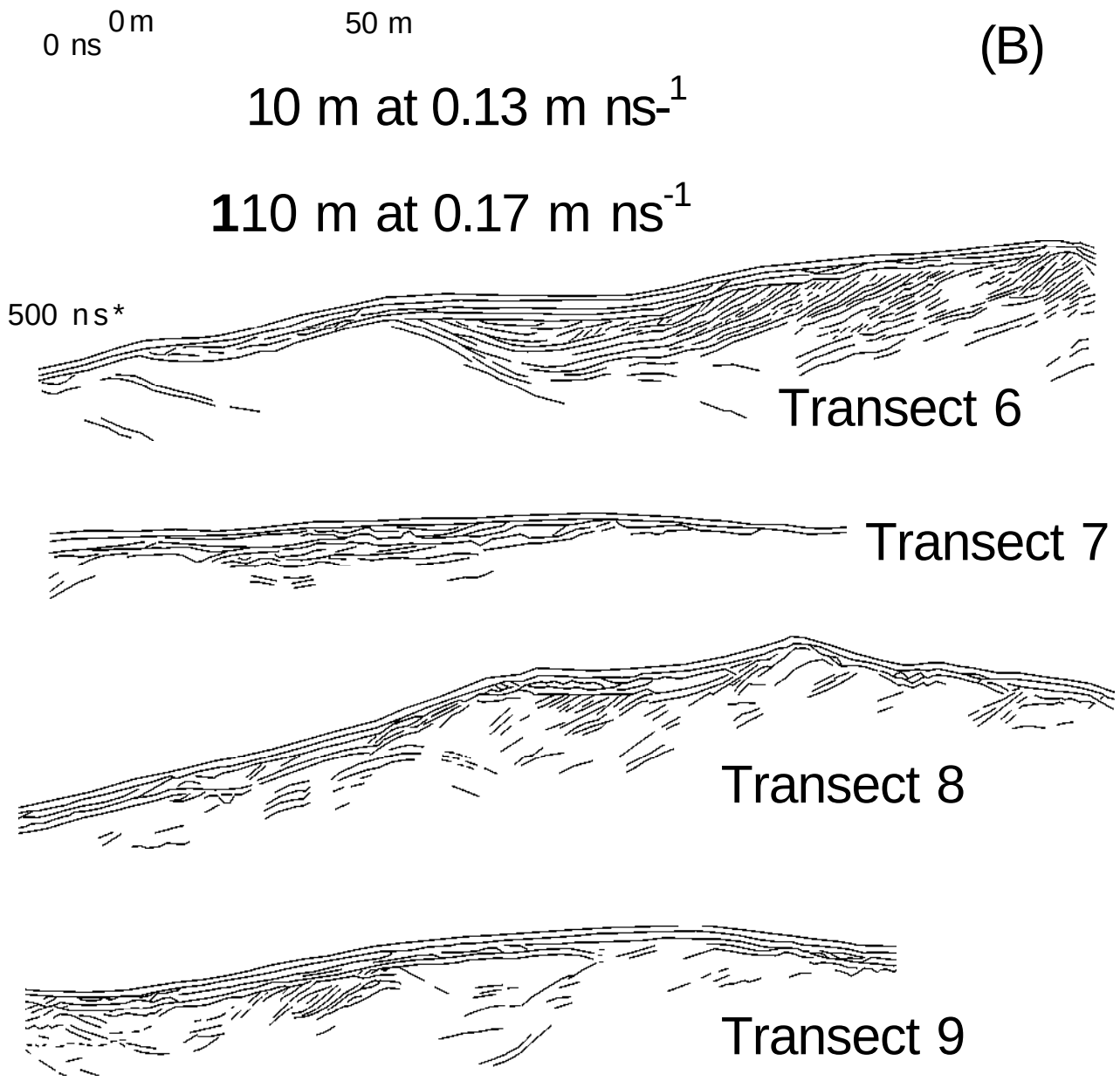

Figure 5 Key reflection characteristics of ground-penetrating radar (GPR) surveys from transects 1–5 (A) and transects 6–9 (B).

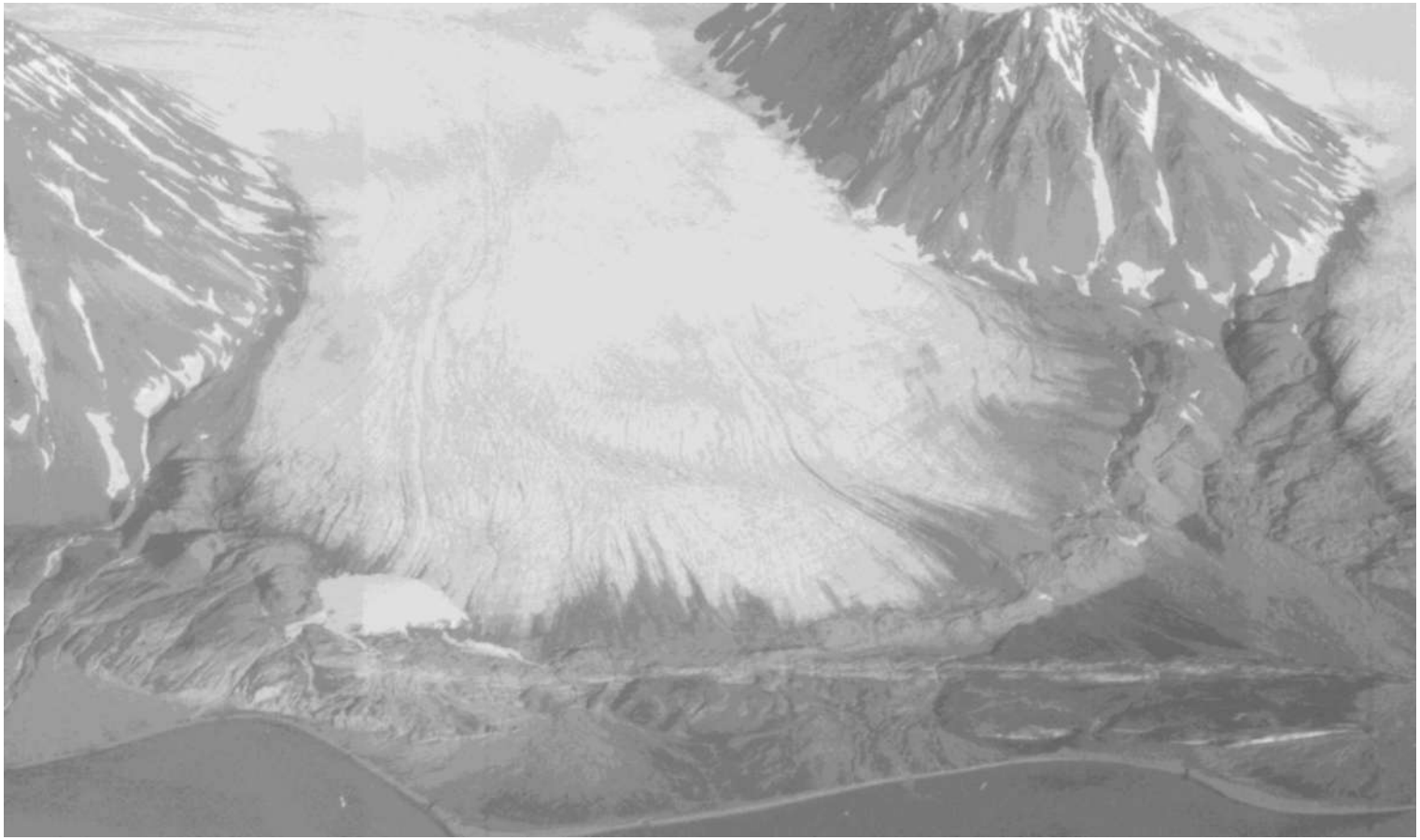

Figure 6 (A) Oblique aerial image of the terminus of Austre Lovénbreen from 1936 imagery (part of aerial photograph S36 1553, published with permission of the Norsk Polarinstitutt); (B) Structural interpretation of Austre Lovénbreen in 1936. The scale varies across the image and associated interpretation, but the widest part of the glacier terminus is around 1.4 km across.

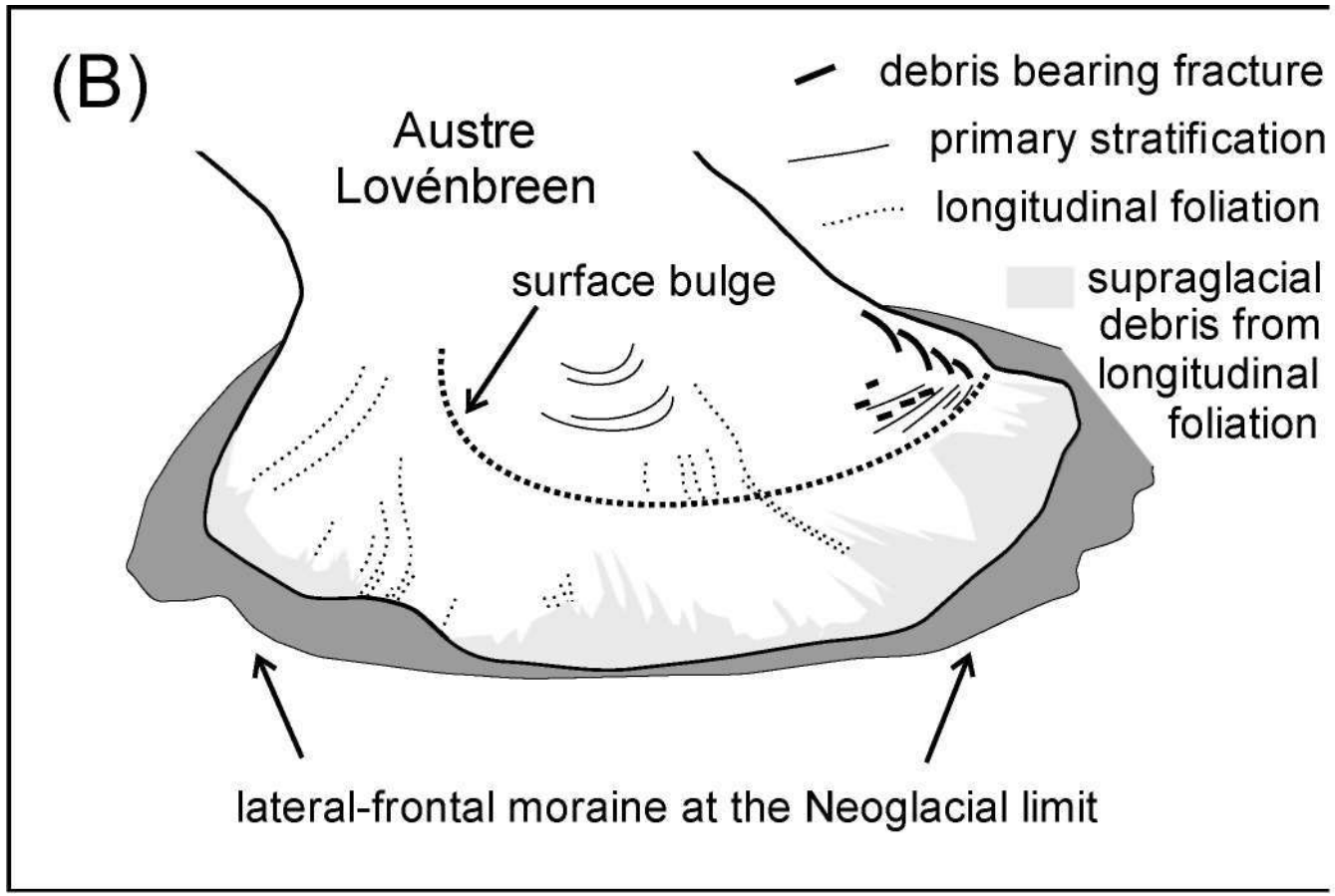

Figure 6 (A) Oblique aerial image of the terminus of Austre Lovénbreen from 1936 imagery (part of aerial photograph S36 1553, published with permission of the Norsk Polarinstitutt); (B) Structural interpretation of Austre Lovénbreen in 1936. The scale varies across the image and associated interpretation, but the widest part of the glacier terminus is around 1.4 km across.

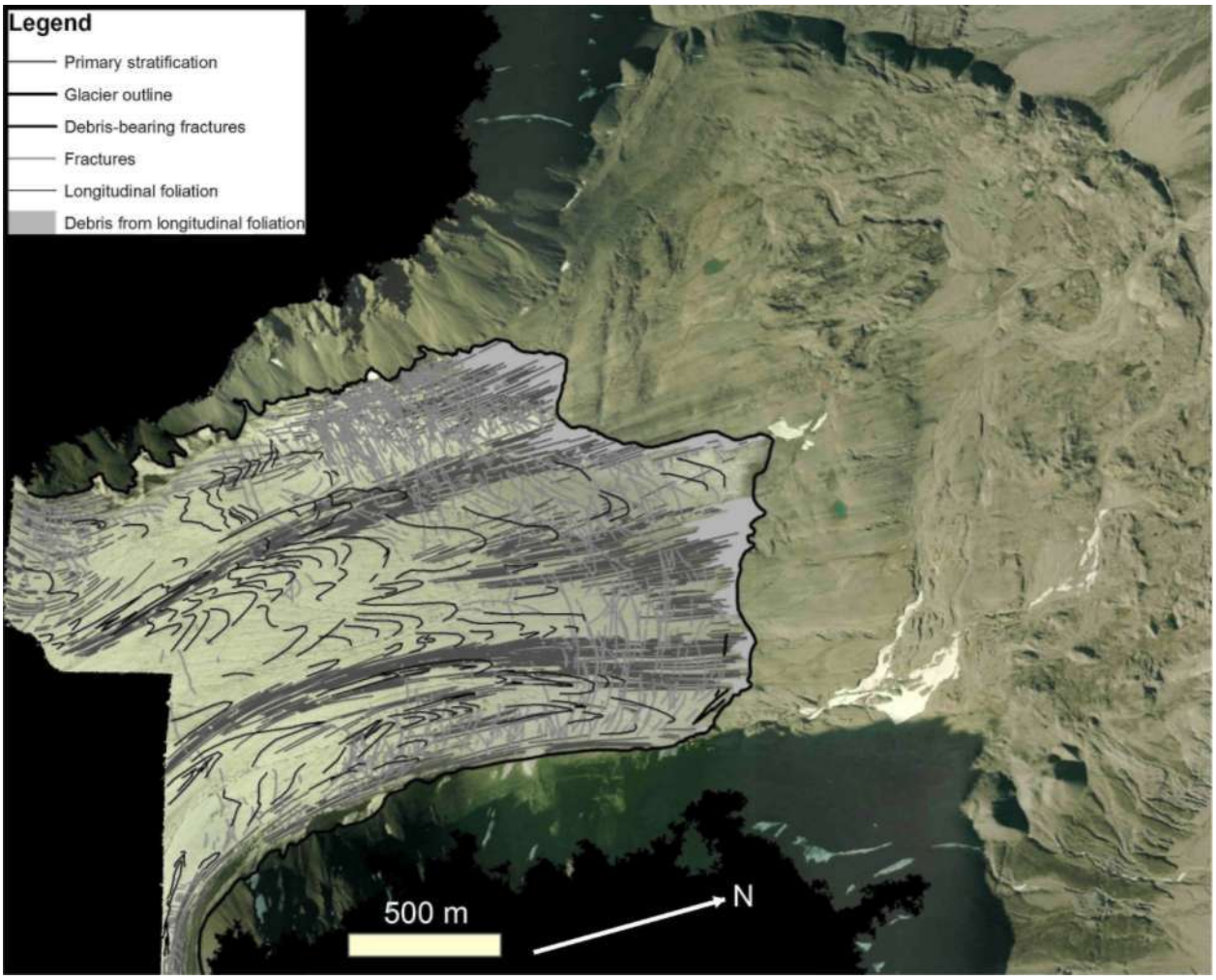

Figure 7 Structural interpretation of Austre Lovénbreen from 2003 imagery. Aerial image data from the UK Natural Environment Research Council (NERC) Airborne Research and Survey Facility (ARSF) are provided courtesy of NERC via the NERC Earth Observation Data Centre (NEODC).